Dendritic LSm1/CBP80-mRNPs mark the early steps of transport commitment and translational control

Alessandra di Penta,[1] Valentina Mercaldo,[1,2,3] Fulvio Florenzano,[1] Sebastian Munck,[2,3] M. Teresa Ciotti,[4] Francesca Zalfa,[1,5] Delio Mercanti,[4] Marco Molinari,[1] Claudia Bagni,[1,2,3,5] and Tilmann Achsel[1,2,3]

[1]Laboratory for Neurobiochemistry, Laboratory for Molecular and Cellular Neurobiology, and Laboratory for Neuroanatomy, Department for Experimental Neurosciences, Fondazione Santa Lucia, Istituto di Ricovero e Cura a Carattere Scientifico, 00143 Rome, Italy
[2]Center for Human Genetics, Katholieke Universiteit Leuven, and [3]Department of Molecular and Developmental Genetics, Flanders Institute for Biotechnology (VIB), B-3000 Leuven, Belgium
[4]Institute for Neurobiology, Consiglio Nazionale delle Ricerche, 00143 Rome, Italy
[5]Department of Experimental Medicine and Biochemical Sciences, Faculty of Medicine, University of Rome "Tor Vergata," 00133 Rome, Italy

Messenger RNA (mRNA) transport to neuronal dendrites is crucial for synaptic plasticity, but little is known of assembly or translational regulation of dendritic messenger ribonucleoproteins (mRNPs). Here we characterize a novel mRNP complex that is found in neuronal dendrites throughout the central nervous system and in some axonal processes of the spinal cord. The complex is characterized by the LSm1 protein, which so far has been implicated in mRNA degradation in non-neuronal cells. In brain, it associates with intact mRNAs. Interestingly, the LSm1-mRNPs contain the cap-binding protein CBP80 that associates with (pre)mRNAs in the nucleus, suggesting that the dendritic LSm1 complex has been assembled in the nucleus. In support of this notion, neuronal LSm1 is partially nuclear and inhibition of mRNA synthesis increases its nuclear localization. Importantly, CBP80 is also present in the dendrites and both LSm1 and CBP80 shift significantly into the spines upon stimulation of glutamergic receptors, suggesting that these mRNPs are translationally activated and contribute to the regulated local protein synthesis.

Introduction

Translational silencing can determine one of several pathways for the messenger RNP (mRNP): first, the mRNP can be kept silent until it is eventually reactivated for translation, mRNA storage. This pathway is particularly well studied in the early developmental stages of insect or amphibian oocytes (Seydoux, 1996). In this case, mRNA silencing is achieved by shortening the poly(A) tail to a critical length that no longer supports translation initiation. Activation of the mRNA consequently involves lengthening of the poly(A) tail in a process that is referred to as "cytoplasmic polyadenylation." In vertebrates, this process requires a characteristic, uridine-rich cytoplasmic polyadenylation element in vicinity to the 3′ end of the mRNA. Cytoplasmic polyadenylation elements are recognized by the cytoplasmic polyadenylation element binding (CPEB) protein, the binding of which causes an inhibition of cap-dependent translation. After a critical phosphorylation, CPEB recruits the cytoplasmic polyadenylation machinery to the mRNA and thereby activates translation (Mendez and Richter, 2001). Another example of mRNA storage is the evolutionarily conserved translational shutdown that occurs in response to cellular stress: the respective signaling cascades cause phosphorylation of the translation initiation factor eIF2α, which blocks translation initiation of most mRNAs at the 48S pretranslational complex (Anderson and Kedersha, 2002).

Second, the silenced mRNPs can be transported to subcellular compartments, to be translated there. Local protein synthesis is very important in polarized cells, as it is crucial for the maintenance of the specialized functions in the respective compartments. This is best exemplified by the neuronal axons and dendrites: in the growing axons, local translation plays a crucial

A. di Penta and V. Mercaldo contributed equally to this paper.

Correspondence to Tilmann Achsel: Tilmann.Achsel@med.kuleuven.be

A. di Penta's present address is Laboratory for Neuroimmunology, Center for Applied Medical Research, University of Navarra, 31080 Pamplona, Spain.

Abbreviations used in this paper: ActD, actinomycin D; CPEB, cytoplasmic polyadenylation element binding; DHPG, (S)-3,5-dihydroxyphenylglycine; DIV, days in vitro; mRNP, messenger RNP; NF-H, neurofilament heavy chain; SMN, survival of motor neurons.

The Rockefeller University Press $30.00
J. Cell Biol. Vol. 184 No. 3 423–435
www.jcb.org/cgi/doi/10.1083/jcb.200807033

role in pathfinding (Piper and Holt, 2004) and is therefore indispensable for the establishing of the proper connections in the nervous system. In the dendrites, synaptic stimulation causes a shift of mRNP components (Steward and Schuman, 2003; Martin and Zukin, 2006; Ferrari et al., 2007) and ribosomes (Ostroff et al., 2002) into the dendritic spines, where translation is activated. The encoded proteins help to modulate the synaptic strength in response to the stimulation, which is the molecular basis of learning and memory. Several proteins have been associated with dendritic mRNAs and implicated in their transport, among them the zip-code binding protein ZBP1 (Zhang et al., 2001), the Fragile X mental retardation protein FMRP (Bagni and Greenough, 2005), and Staufen (Köhrmann et al., 1999; Villacé et al., 2004). Despite this knowledge, the process of selection of dendritic mRNAs and their transport into the dendrites remains largely enigmatic.

Finally, the silenced mRNA can be degraded. Regulated mRNA degradation frequently starts with deadenylation, either through consecutive shortening of the poly(A) tail or by an endonucleolytic cleavage in the 3′ UTR. Deadenylation at the 3′ terminus then causes decapping at the 5′ end and 5′→3′ exonucleolytic degradation (Meyer et al., 2004). In addition to the decapping enzyme and the exonuclease, the process requires the activity of several auxiliary factors, such as the seven LSm proteins, LSm1–7. The LSm proteins associate with the mRNAs that are targeted for degradation (Tharun and Parker, 2001) and are required for efficient decapping in yeast (Tharun et al., 2000). In mammals, the LSm proteins act upstream of the degrading enzymes (Cougot et al., 2004; Andrei et al., 2005) and are probably involved in translational silencing before degradation (the LSm1-associated factor Pat1p inhibits translation in yeast [Coller and Parker, 2005]). The LSm ("Like Sm") proteins take their name from a sequence homology to the Sm proteins that constitute the core of the spliceosomal small nuclear RNP complexes: they are essential pre-mRNA splicing factors. Similarly, all characterized LSm proteins are involved in various steps of mRNA metabolism. The Sm/LSm proteins share a common domain that is responsible for the fact that seven family members form a circular complex. In vivo assembly of the Sm complex proper requires catalysis by the survival of motor neurons (SMN) protein and associated factors (Meister et al., 2002). Insufficient expression of SMN causes a selective degeneration of α motor neurons, a condition called spinal muscular atrophy. How insufficiency of a general splicing factor can have such a selective effect remains enigmatic; possibly SMN has a second function. LSm4 has been implicated because it contains the high affinity SMN-binding domain that is also found in the Sm proteins (Brahms et al., 2001; Friesen et al., 2001), but none of the processes that require LSm proteins is specific for neurons.

mRNA silencing by any of the aforementioned mechanisms can coincide with aggregation of the respective mRNPs into cytoplasmic granules: the polar granules in the case of maternally stored mRNAs in insects, the stress granules in case of stress-induced shutdown of translation, the transport granules in the case of mammalian dendritic transport, and the P bodies in the case of mRNAs that undergo degradation. The distinction between the various types of mRNA granules is not always clear: P bodies are on the one hand mRNA degradation centers, on the other hand they can also store stress-silenced mRNAs in yeast (Brengues et al., 2005) and microRNA-silenced mRNA in higher eukaryotes (Filipowicz et al., 2008). In insects, there appears to be a huge overlap between P body markers and neuronal transport granules (Barbee et al., 2006).

Here, we show that the auxiliary mRNA degradation factor LSm1 has a second function in neurons in that it forms stable dendritic mRNPs. The LSm1 mRNPs contain the CBP80 subunit of the nuclear cap-binding complex, indicating that the localized mRNP was assembled in the nucleus, thus linking mRNA transport to nuclear events. In support of this notion, the otherwise predominantly cytoplasmic protein LSm1 becomes partially nuclear upon inhibition of novel mRNA synthesis and hence export. Further, LSm1 mRNPs contain the cytoplasmic polyadenylation element binding factor CPEB. Finally, we show that both CBP80 and LSm1 migrate into the spines after mGluR stimulation, a typical sign of their regulated activation.

Results

The LSm proteins localize in the dendrites in vitro and in vivo

As we were interested in the expression of the auxiliary mRNA degradation factors LSm1 to LSm7 in the neuronal system, we looked at the subcellular localization of the LSm proteins in primary neuronal cells. We used antibodies directed against LSm1 (Ingelfinger et al., 2002; Fig. S1, available at http://www.jcb.org/cgi/content/full/jcb.200807033/DC1). Primary neurons were prepared from two different rat tissues, namely the spinal cord and the cerebellum, and labeled with affinity-purified α-LSm1 antibodies. To identify the neurons and at the same time reveal the neurites, the slides were counterstained with a monoclonal α-MAP2 antibody. As shown in Fig. 1, neurons derived from the spinal cord (Fig. 1, A–D) show a prominent, punctuated signal for LSm1 in the cell body (Fig. 1 A, arrow), probably the mRNA-degrading P bodies. In addition, LSm1 is also highly expressed in the dendrites (Fig. 1 A, arrowhead), which is shown by the colocalization with the dendritic marker MAP2 (Fig. 1 C, yellow), thus confirming and extending a recent observation (Vessey et al., 2006). As we used affinity-purified antibodies, we were able to determine the LSm1 distribution with high resolution: the dendritic LSm1 is present in apparently granular structures (Fig. 1 D). The spinal cord neurons were not further separated, and motor neurons and interneurons as well as glia cells are present. All neurons have LSm1 present in the neurites (unpublished data). Moreover, when spinal cord neurons were grown in the presence of FBS, the neurons tended to cluster and send bundles of multiple neurites to nearby cell clusters. In these bundles, the granular structure of the LSm1 signal becomes very evident (Fig. 1, E–H, the MAP2-positive cell in the middle lies on top of the bundle and the MAP2-negative cell at the right is presumably a glial cell).

Rat cerebellar cells were cultured to enrich the Purkinje neurons and their identity was verified by staining for Calbindin that, in cerebellum, marks the dendrites specifically of the Purkinje cells (unpublished data). As for the spinal cord neurons, LSm1 is highly present in the dendrites (Fig. 1 I).

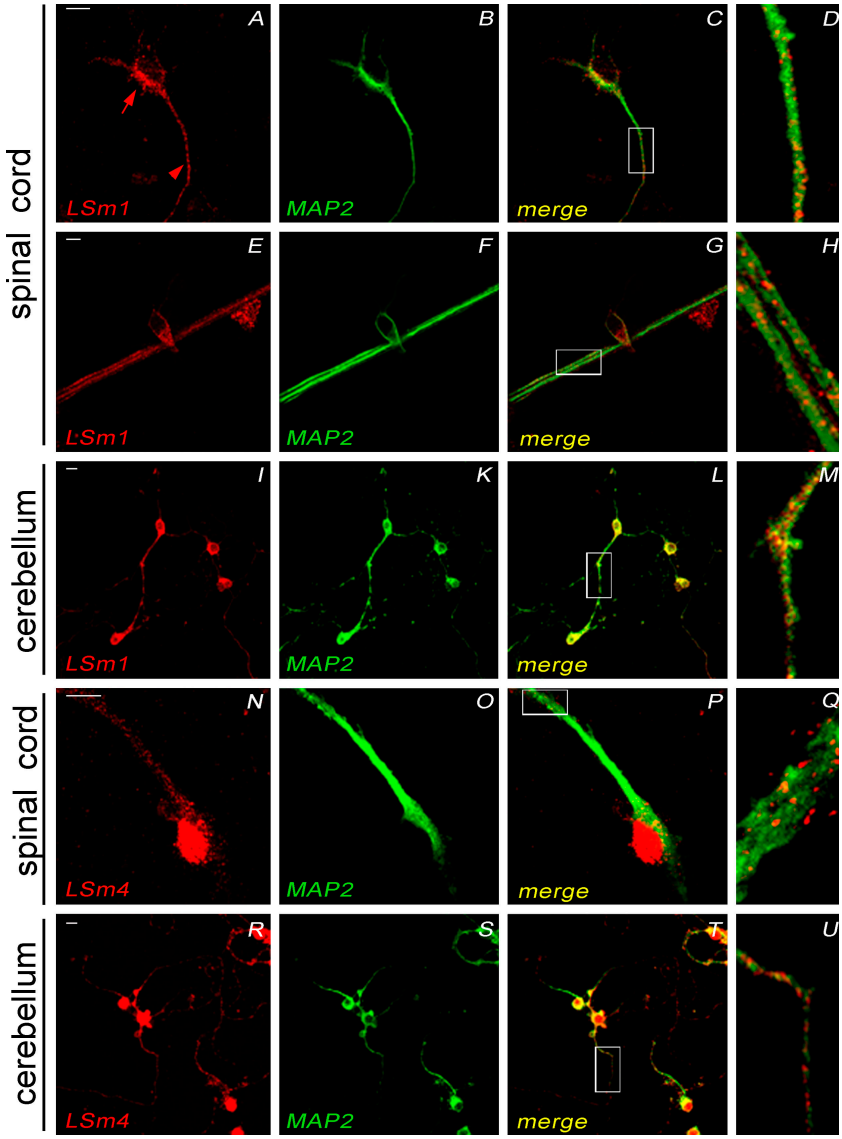

Figure 1. **LSm1 and LSm4 localize in the neurites of primary neurons.** Rat spinal cord neurons were cultured in the presence of B27 supplement (A–D and N–Q) or of serum (E–H) for 7 DIV; cerebellar Purkinje cells were cultured as described in Materials and methods for 7 DIV (I–M and R–U). Cells were stained with monoclonal α-MAP2 antibody (green) and polyclonal α-LSm1 (A–M, red) or α-LSm4 antibodies (N–U, red). Shown are confocal micrographs of the separated channels and the merged images. Red arrow (LSm1 in the cell body) and arrowhead (in the dendrites) indicate regions of interest as described in the text. White boxes indicate the area enlarged in the subsequent panel. Bars, 10 μm.

To determine whether other components of the LSm complex are also present in the neurites, we stained primary neurons with affinity-purified α-LSm4 antibodies, again counterstaining with the α-MAP2 antibody. As expected, we observed a very prominent signal in the nucleus of the neurons, because LSm4 is not only part of the cytoplasmic LSm1-7 complex but also of the nuclear U6 small nuclear RNP (Achsel et al., 1999). In addition, LSm4 is clearly visible also in the neurites of both spinal cord neurons (Fig. 1 Q) and in Purkinje cells (Fig. 1 U). In conclusion, we found the LSm proteins in the cell body of various neurons where they presumably have the same roles as in immortalized cell lines: mRNA splicing in the nucleus and mRNA degradation in the cytoplasm. In addition, the LSm proteins are present in the neurites of the cells, the function of which is not immediately clear.

Next, we investigated the distribution of LSm1 proteins in the rat central nervous system in vivo. LSm1 is expressed throughout the central nervous system with positive cells of different size and shape present in virtually all areas. Exemplarily, sections from the cerebral cortex and the cerebellum are shown in Fig. 2 A. In the cerebral and cerebellar cortices, all LSm1-positive cells are characterized by a granular distribution of the staining, which is often present also at considerable distances from the cell bodies (Fig. 2 A, a, d, and g). Double labeling with LSm1 and different markers (neurofilament heavy chain [NF-H], SMI31, or SMI 32) capable to evidence both neuronal dendrites and axons show a significant localization of LSm1 in these neuronal processes (dendrites are shown by arrowheads in Fig. 2 A, d). In the cerebral cortex as well as in the cerebellum, both large neurons, pyramidal and Purkinje cells, as well as small ones, possibly interneurons, are LSm1 positive. Furthermore, double labeling with the marker glial fibrillary acidic protein (unpublished data) suggests that glial cells also express LSm1. Expression of LSm1 in neuronal cell bodies and dendrites is present throughout the brain: double labeling of LSm1 with different specific markers demonstrates its presence in the cerebellar cortex (Fig. 2 A, g–i), as well as in hippocampus, thalamus, hypothalamus, and substantia nigra pars compacta (Fig. S2, available at http://www.jcb.org/cgi/content/full/jcb.200807033/DC1). Interestingly, no expression of LSm1 is present in the presynaptic

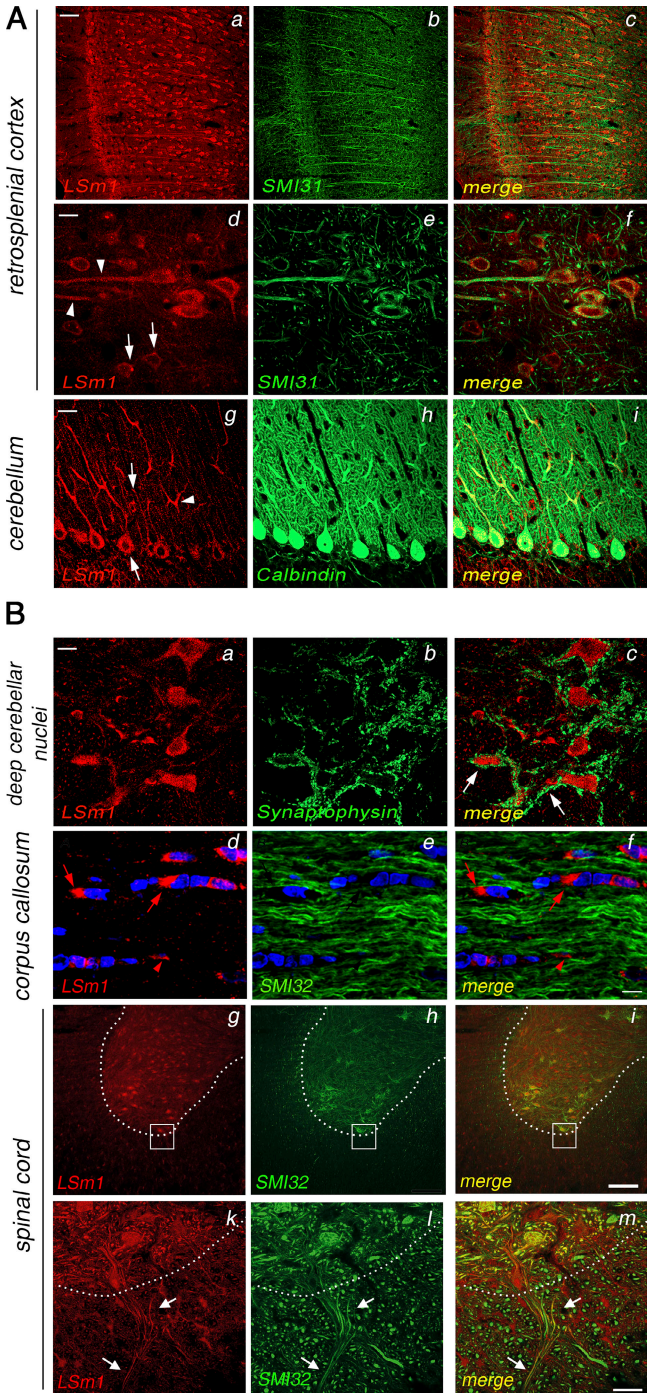

Figure 2. **LSm1 localizes in vivo in neuronal cell bodies and neurites.** (A) LSm1 is found in dendrites. Rat brain slices were stained with α-LSm1 (a, d, and g) as well as with the α-neurofilament antibody SMI31 (b and e) or α-Calbindin (h). Images were acquired by confocal microscopy. Shown are the retrosplenial granular cortex (a–f) and the cerebellar cortex (g–i). (d) Arrowheads highlight α-LSm1–positive granular structures in pyramidal neurons and arrows point to similar structures in small cells. (g) Arrows point to α-LSm1–positive granular structures in Purkinje cells and interneurons and arrowheads show similar structures in the dendritic tree of the Purkinje cells. Bars: (a) 100 µm; (d) 20 µm; (g) 40 µm. (B) LSm1 is found only in some axonal structures. Shown are the deep cerebellar nuclei (a–c), the corpus callosum (d–f), and a transversal section of the spinal cord (g–m); k–m shows the detail boxed in g–i. The sections were stained with α-LSm1 (a, d, g, and k), α-synaptophysin (b), and α-NF-H (SMI32 antibody; e, h, and i). White arrows (c) point to presynaptic structures void of LSm1 signal and red arrows (d and f) point to α-LSm1 immunoreactivity associated with cell nuclei. The dashed line in g–m indicates the gray-to-white matter boundary and white arrows point to LSm1 signals present in neurofilament-positive fibers, presumably axons, in the white matter. Bars: (a) 20 µm; (f) 10 µm; (i) 200 µm; (m) 30 µm.

terminals, at least of the deep cerebellar nuclei. As shown in Fig. 2 B (a–c), LSm1 is well expressed in the cell bodies, but does not colocalize with the presynaptic marker synaptophysin that surrounds the neurons (Fig. 2 B, green in the merged image and white arrows). In axons, LSm1 labeling is not consistent. This is exemplified by differences between the LSm1 labeling in the corpus callosum, one of the major fiber tracts of the brain, and in the spinal cord. In the corpus callosum, only interspersed cell bodies exhibit LSm1 signals next to the nuclei (Fig. 2 B, d and f, red arrows; the nuclei are highlighted by blue DAPI staining), whereas fibers, indicated by NF-H labeling of axons, do not colocalize with LSm1 (Fig. 2 B, f). In the spinal cord, the picture is different. Fig. 2 B (g–i) shows an overview over a transversal section, with the gray matter outlined by a dashed line. Both cell bodies and dendritic structures in this area express LSm1 as well as NF-H. Zooming in on the ventral border of the gray matter, it becomes evident that axonal fibers in the white matter also express LSm1 (Fig. 2 B, k–m, white arrows). As this is the region where axons leave toward the ventral root, these structures can be tentatively identified as the axons of α motoneurons. In conclusion, LSm1 is expressed in glial and in many neuronal cell types, and it is present, albeit to varying degrees, in dendrites. As regards to axons, in contrast, LSm1 has been clearly localized only in spinal cord fibers.

LSm1 is part of stable mRNPs

As the LSm proteins are involved in mRNA metabolism, it was tempting to speculate that the dendritic LSm1 population also associates with mRNAs. To test this notion, we performed immunoprecipitation experiments with affinity-purified α-LSm1 antibodies, using total rat brain extracts. RNAs that coprecipitate with LSm1 were isolated, and the presence of specific mRNAs was revealed by RT-PCR. We tested four mRNAs that are known to be localized in neurites (Steward and Schuman, 2003; Tsokas et al., 2005), namely the mRNAs coding for β-actin, MAP1B, CaMKIIα, and eEF1α1. As shown in Fig. 3 A, all four mRNAs coprecipitate with LSm1 (lanes 3, 6, 9, and 12) but not in the precipitation with unspecific IgGs (lanes 2, 5, 8, and 11). We conclude that, in rat brain extracts, LSm1 stably associates with mRNPs that have been reported to localize in the dendrites. To test whether LSm1 directly binds to the mRNAs in the rat brain, we used a cross-linking/immunoprecipitation protocol (Ule et al., 2003). Under the highly stringent conditions of the RIPA buffer, most protein–protein and protein–RNA interactions are broken, and mRNAs did not coprecipitate with LSm1 (Fig. 3 B, lane 2). When the tissue is UV irradiated before extract preparation, mRNAs that are in molecular contact are covalently linked to LSm1 and therefore coprecipitate even under stringent conditions (Fig. 3 B, lanes 3 and 4). Therefore, the UV-dependent precipitation of the β-actin, MAP1B, and eEF1α1 mRNAs demonstrates that these molecules are in direct contact

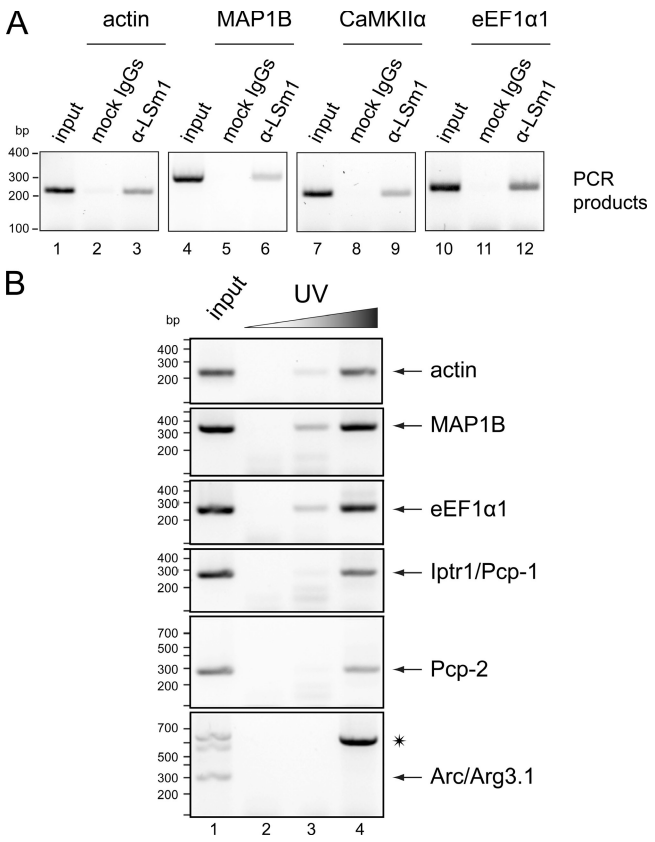

Figure 3. **LSm1 binds stably and directly to mRNAs.** (A) Immunoprecipitations were performed from rat brain extracts with affinity-purified α-LSm1 antibodies (lanes 3, 6, 9, and 12) or with an equal amount of nonspecific IgGs (lanes 2, 5, 8, and11). Coprecipitated RNA was isolated and analyzed by RT-PCR using oligos specific for the β-actin, MAP1B, CaMKIIα, and eEF1α1 mRNAs. Shown is the product of the PCR reactions. In lanes 1, 4, 7, and 10, RT-PCR was performed on 1/50 of the extract used in each precipitation. The migration of DNA markers is indicated on the left. (B) Rat brain was UV irradiated for 0, 45, and 90 s (lanes 2–4), extract was prepared as before, and LSm1 immunoprecipitations were performed under semidenaturing conditions. Coprecipitating mRNAs were visualized by RT-PCR with primers specific for β-actin, MAP1B, eEF1α1, Iptr1/Pcp-1, Pcp-2, and Arc/Arg3.1 as indicated. The RT-PCRs in lane 1 was performed on 1/100 of the supernatant of lane 2. The asterisk in the bottom panel marks a band that runs at the height expected for the product of the Arc/Arg3.1 pre-mRNA. The migration of DNA markers is indicated on the left of each panel.

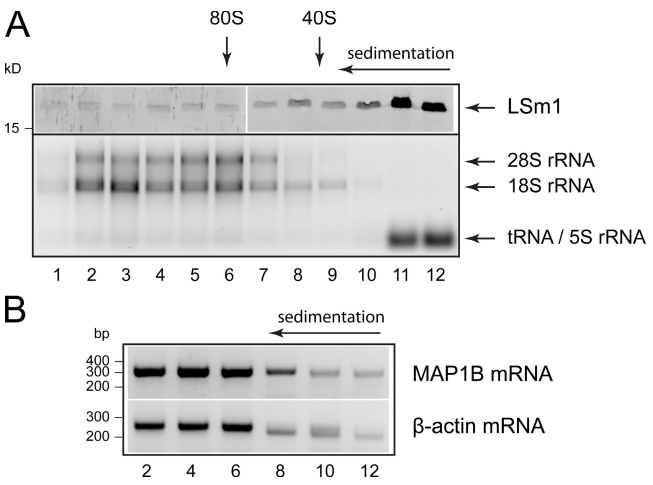

Figure 4. **Characterization of the LSm1 mRNP by sucrose gradient centrifugation.** (A) Rat brain extract was fractionated by sucrose gradient centrifugation. The distribution of LSm1 protein was analyzed by SDS-PAGE and Western blotting (top) and the distribution of the major RNAs was analyzed by agarose gel electrophoresis and ethidium bromide staining (bottom). The migration of a molecular mass marker is indicated on the left of the top panel. (B) Rat brain extract was UV irradiated, and then fractioned by sucrose gradient centrifugation. Even-numbered fractions were diluted with RIPA buffer and precipitated with α-LSm1 antibodies. Coprecipitating MAP1B mRNAs (top) and β-actin (bottom) were detected by RT-PCR. PCR products were separated on agarose gels and ethidium bromide stained. The migration of DNA markers is indicated on the left.

with LSm1 (Fig. 3 B, first three panels). We further checked for the coprecipitation of other dendritic mRNAs: the IP_3 receptor Iptr1/Pcp-1 and the Purkinje cell protein Pcp-2 are highly expressed in the Purkinje cells and their mRNA is also dendritic (Iijima et al., 2005). Both mRNAs cross-link to LSm1 (Fig. 3 B, fourth and fifth panels) in agreement with the notion that LSm1 in the dendrites associates with mRNAs. Arc/Arg3.1, finally, is an mRNA that localizes in hippocampal dendrites and that is regulated by nonsense-mediated mRNA degradation (Giorgi et al., 2007). Because LSm1 is an auxiliary mRNA degradation factor, even though it is not implicated in nonsense-mediated decay, we checked for association with this mRNA. Arc mRNA is not detected in the immunoprecipitate, showing the specificity of the method (Fig. 3 B, sixth panel); only a longer fragment is detected, the length of which corresponds to the Arc/Arg3.1 pre-mRNA (Fig. 3 B, asterisk).

To characterize the LSm1 mRNP biochemically, we loaded the brain extract (virtually void of nuclei) on sucrose gradients to separate complexes by size. Extract preparation and gradient conditions were established to give an optimal yield and spread of the LSm1 protein (Fig. 4 A, top). It was not intended to infer association with polysomes from the sedimentation velocity, and the distribution of ribosomes (Fig. 4 A, bottom) was analyzed solely to estimate the size of complexes present in the various fractions (indicated at the top of Fig. 4 A). The bulk of LSm1 sediments in the two top fractions, indicating a very small complex, if not monomeric protein. In addition, detectable LSm1 levels are observed in all fractions, which corresponds to complexes of up to 80S and more. To determine the size of the LSm1 mRNP, extracts were irradiated with UV light before loading onto the sucrose gradient. Even-numbered fractions were immunoprecipitated under the stringent conditions used in Fig. 3 B to reveal the sedimentation of mRNPs where LSm1 is in molecular contact with the pre-mRNA. The strongest signal for both MAP1B and β-actin mRNA is obtained in the bottom half of the gradient, where LSm1 is underrepresented. In the top half, and especially in the top fraction where LSm1 is most abundant, the signal is much weaker (Fig. 4 B). Thus, only a small percentage of LSm1 is assembled, at steady state, into large mRNPs.

LSm1 mRNPs contain the CPEB protein and the nuclear cap-binding protein CBP80

To further characterize the composition of the LSm1 mRNPs, we coupled the sucrose gradient centrifugation with an immunoprecipitation step. The above gradients (without UV irradiation) were arbitrarily divided into three pools of fractions:

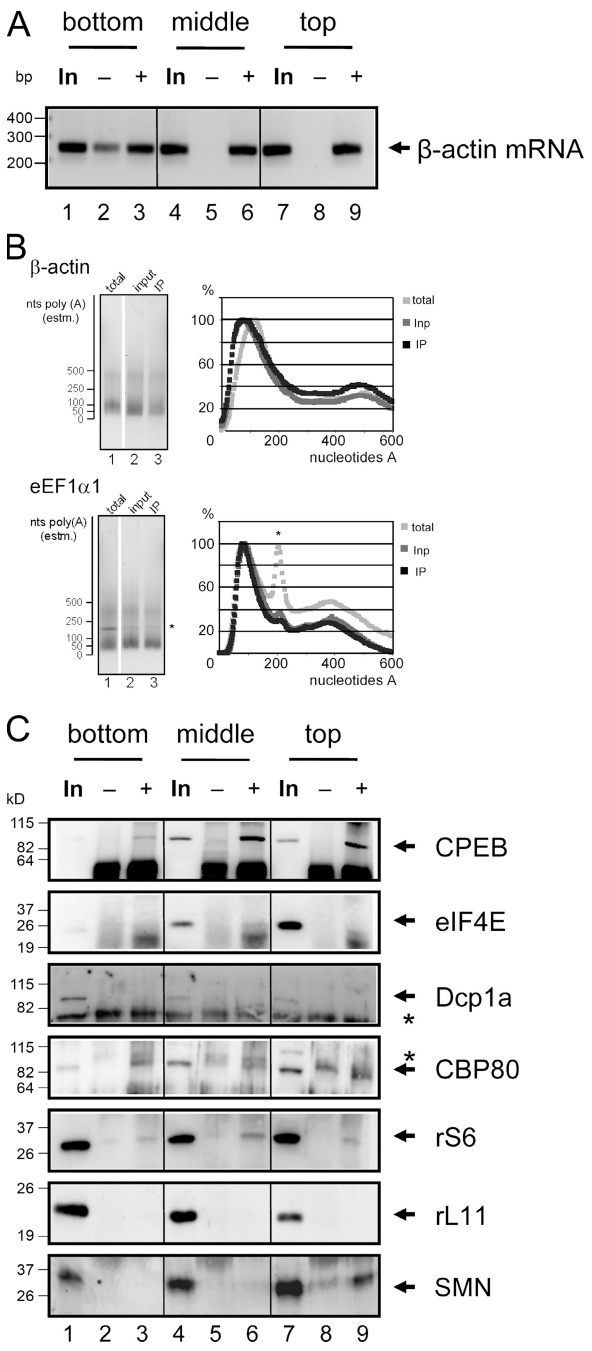

Figure 5. **LSm1 mRNPs contain polyadenylated mRNAs, CPEB, and CBP80.** (A) Rat brain extracts were separated as before and three fractions were collected: bottom (equivalent to fractions 2–4 in Fig. 4 A), middle (fractions 5–7 in Fig. 4 A), and top (fractions 8–10 in Fig. 4 A). mRNP complexes were immunoprecipitated with mock IgGs (lanes 2, 5, and 8) or with α-LSm1 antibodies (lanes 3, 6, and 9). Lanes 1, 4, and 7 show the RT-PCR of 2.5% of the respective inputs. RNA was isolated and β-actin mRNA was detected by RT-PCR. PCR products were analyzed by agarose gel electrophoresis and ethidium bromide staining; DNA markers are indicated on the left. (B) β-Actin and eEF1α1 mRNAs were amplified from a pool of the three fractions (lanes 2 and 3) or from total RNA isolated from the crude brain extract (lane 1) by the tag-addition poly(A) test (Fig. S2, available at http://www.jcb.org/cgi/content/full/jcb.200807033/DC1). The lanes were scanned and the intensity is plotted on the right. The y axis gives the signal intensity relative to the peak of each lane. On the x axis, the position is plotted. Approximate poly(A) tail lengths were estimated from the molecular markers and the length of the amplicons without poly(A). The asterisk in the eEF1α1 panel indicates an artifact that is not dependent on tagging of the mRNA (Fig. S2). (C) Proteins were isolated from the three fractions immunopurified as in A, and the following proteins were detected by Western blotting (from top to bottom): CPEB, eIF4E, Dcp1a, CBP80, rS6, rL11, and SMN. The position of the specific bands are indicated by arrows on the right and the migration of molecular mass markers on the left; asterisks designate bands that derive from the antibodies used in the immunoprecipitations and that are therefore present in high concentration on the blot. Lanes 1, 4, and 7 show the input (10% of the immunoprecipitated material), lanes 2, 5, and 8 the mock precipitation with nonspecific IgGs, and lanes 3, 6, and 9 the specific α-LSm1 immunoprecipitations.

bottom (fractions 2–4), middle (fractions 5–7), and top (fractions 8–10). The last two fractions were discarded, thus eliminating the major part of LSm1 that is not incorporated into complexes of meaningful size and that would only cause background in the following analysis. After α-LSm1 immunoprecipitation, copurifying β-actin mRNA was revealed by RT-PCR. Fig. 5 A shows that the β-actin mRNA is present in all three regions of the gradient (lanes 1, 4, and 7) and strongly coprecipitates with LSm1 (lanes 3, 6, and 9). Immunoprecipitation with mock IgGs yielded little (Fig. 5 A, lane 2) or no background signal (Fig. 5 A, lanes 5 and 8); the little background in lane 2 is caused by the fact that the signal in the bottom fraction was stronger than in the other two, resulting in saturated bands for input and immunoprecipitation and detection of the slight background.

mRNAs are stabilized by the presence of the poly(A) tail. It was therefore interesting to detect the poly(A) tail and measure its length, which also gives some indication to the translational status. Available methods for poly(A) length measurement are all rather inefficient and require substantial amounts of RNA, more than can be obtained in immunoprecipitations. We therefore devised a new method that uses a Klenow fill-in reaction to tag the poly(A) tail with a specific sequence and that works with low amounts of RNA (the method is described in Fig. S3, available at http://www.jcb.org/cgi/content/full/jcb.200807033/DC1). Analysis of sucrose gradient/immunoprecipitation double-purified actin mRNAs shows that, similar to the input mRNAs, the poly(A) length shows a bipartite distribution, with the majority of the signal in a peak that corresponds to 50–100 nucleotides of poly(A). A second peak corresponds to >200 nucleotides. A similar picture is observed for the eEF1α1 mRNA (Fig. 5 B, bottom), and the mRNAs isolated from the bottom and middle fractions also show very similar distributions (not depicted). To quantify the result, the signal intensity along the respective lanes was plotted against the position on the gel. The corresponding poly(A) tail lengths were estimated from the molecular mass markers present on the same gel and are indicated on the x axis. As can be seen on Fig. 5 B (right), the profile does not significantly change. All mRNAs have poly(A) tails that are long enough to exclude ongoing mRNA degradation.

CPEB1 is present on dendritic mRNPs, regulates translation, and also modulates poly(A) tail length (Mendez and Richter, 2001). LSm1-associated proteins were purified by sucrose gradient/immunoprecipitation as above and analyzed by Western blotting. CPEB1 was specifically present in LSm1 complexes from all three regions of the sucrose gradient (Fig. 5 C, top),

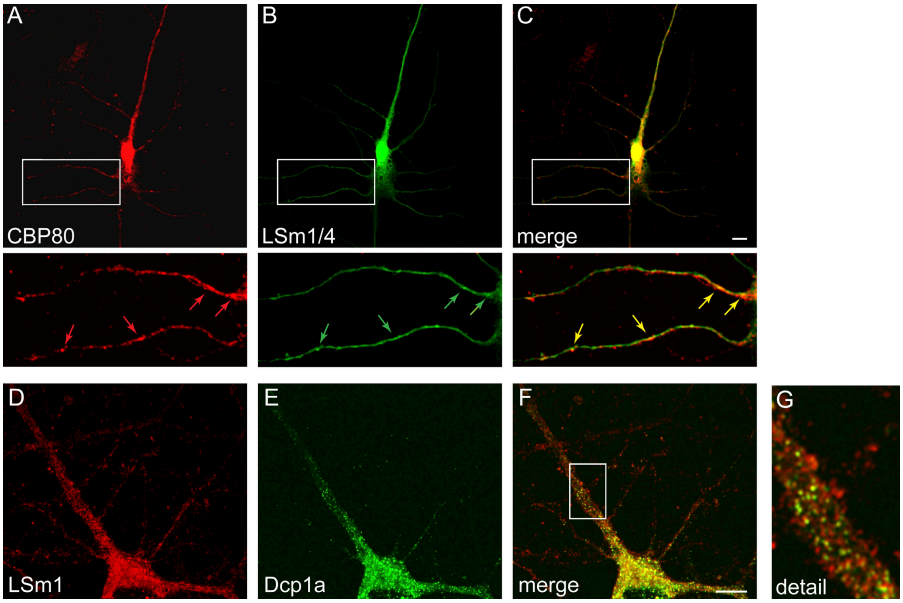

Figure 6. **Dendritic LSm1 colocalizes with CBP80, but not with hDcp1a.** Hippocampal neurons (10 DIV) were transfected simultaneously with YPet-LSm1 and YPet-LSm4 and counterstained with α-CBP80 antibodies (A–C) or transfected with YPet-hDcp1a and counterstained with α-LSm1 (D–G). The cells were further stained with α-MAP2 to confirm their neuronal identity (not depicted). Shown are confocal optical slices. The YFP channel is shown in green and the antibodies in red. The right column shows the merged picture. The details highlighted in A–C are shown below the respective panels; the detail in F is shown in G. Bars, 10 µm.

indicating that LSm1 mRNPs indeed have the potential to be activated by cytoplasmic polyadenylation.

Further, functional mRNAs have an m^7G cap structure at their 5′ terminus, which is bound by the translation initiation factor eIF4E. eIF4E is present mainly in the top fraction (Fig. 5 C, second panel, lane 7), and only minor amounts are found in the middle part of the gradient (Fig. 5 C, second panel, lane 4). In none of the fractions eIF4E precipitated with LSm1 (Fig. 5 C, lanes 3, 6, and 9). If eIF4E is not bound to the cap, the decapping enzyme that competes with eIF4E may be present on the mRNP. The Dcp1a subunit of the enzyme is found in all three fractions of the gradient (Fig. 5 C, third panel, lanes 1, 4, and 7), but it does not coprecipitate with LSm1. Probably, the P bodies in the cell bodies that contain LSm1 and Dcp1a disintegrate during the purification scheme. That leaves only the nuclear cap-binding complex, which binds to the cap during maturation of the mRNA and its export from the nucleus. We verified the presence of the bigger subunit CBP80: it was detected in all three zones of the gradient and it coprecipitated with LSm1 in significant amounts in all three fractions (Fig. 5 C, fourth panel). We conclude that the LSm1 mRNPs have CBP80 bound to the 5′ cap structure.

To further characterize the LSm1-associated mRNPs, we investigated association with translational markers. FMRP, an important neuronal and dendritic translational regulator (Napoli et al., 2008), does not coprecipitate with LSm1 and colocalizes only to a very small extent with dendritic LSm1 (unpublished data). The ribosomal protein S6 coprecipitated in all three regions of the gradient, indicating association with the small ribosomal subunit (Fig. 5 C, fifth panel). The large ribosomal subunit protein L11, instead, is not significantly associated with LSm1 mRNPs (Fig. 5 C, sixth panel), suggesting the presence of stalled 48S initiation complexes. Finally, the LSm complex interacts, at least in vitro, with SMN (Friesen and Dreyfuss, 2000; Brahms et al., 2001). The interaction is confirmed in the brain extract (Fig. 5 C, seventh panel). It should be noted, however, that the interaction is mostly restricted to the top fraction containing the lightest complexes, as if SMN is part only of a subset of LSm1 complexes.

Dendritic LSm1 colocalizes with CBP80, but not Dcp1a

So far, we have biochemically characterized a stable LSm1 complex that contains several mRNAs that are also found in the dendrites. To demonstrate that the complex actually is dendritic, we studied the subcellular localization of the involved proteins in primary neurons. We know that LSm1 resides in the dendritic compartment (Figs. 1 and 2), and the same is true for CPEB and eIF4E (Huang et al., 2003; Smart et al., 2003). We therefore looked at the cap-binding protein in our complex. In primary neurons, CBP80 is detected in the cell bodies and in particular in the nucleus, as expected. Significantly, it is clearly also present along the dendrites (Fig. 6 A). We expressed fluorescent versions of the LSm proteins (tagged with YPet; Nguyen and Daugherty, 2005) and coexpressed LSm1 and LSm4 because LSm subcomplexes give more specific localization signals (Ingelfinger et al., 2002). We further used a neuron-specific promoter to better control expression levels and better reveal cellular structures. The resulting pattern faithfully reproduces the localization of the endogenous LSm1 and LSm4 proteins (compare Fig. 6 B with Fig. 1). Significantly, several dendritic spots of LSm1/4 enrichment coincide with CBP80 foci (Fig. 6 C, yellow arrows). Further, we transfected with YPet-Dcp1a and counterstained with α-LSm1 antibodies. YPet-Dcp1a is expressed in granular structures in the cell body (Fig. 6 E) that colocalize with LSm1 and therefore appear as bright yellow spots in the merged image. These structures presumably correspond to the mRNA-degrading P bodies that were observed in undifferentiated cell lines (Ingelfinger et al., 2002; Cougot et al., 2004). Note that P bodies are not homogenous macromolecular complexes and colocalization of LSm1 and Dcp1a in the cell body therefore does not contradict our finding that they do not

interact (Fig. 5 C). Outside the cell body, the two proteins segregate: Dcp1a granules contain little or no LSm1 and thus appear green in the merged image (Fig. 6 G). We conclude that LSm1 granules in the dendrite contain CBP80, but no Dcp1a. In the cell body, they mostly contain Dcp1a. The biochemically characterized LSm1 particles (Fig. 5) therefore most likely represent the dendritic fraction.

LSm1-CBP80 accompanies the mRNAs from the nucleus to the spines

The presence of the nuclear cap-binding protein in the LSm1 mRNP may suggest that the complex is assembled in the nucleus before exit to the cytoplasm. LSm1 has so far been described as entirely cytoplasmic. Careful inspection of LSm1-stained primary neurons, however, revealed some nuclear staining with certain variability between cells (Fig. 7 and not depicted), indicating that LSm1 is not rigorously excluded from the nucleus. The predominantly cytoplasmic localization in the steady state could then be driven by the efficient transport of newly synthesized mRNAs into the cytoplasm. To test this hypothesis, we inhibited de novo synthesis of mRNAs, and hence mRNA export to the cytoplasm, by actinomycin D (ActD) treatment of primary hippocampal neurons for 3 h. Fig. 7 shows the projection of confocal slices that span the entire cell. A typical cell in the untreated sample (Fig. 7 A, top) shows only a faint LSm1 signal (red) that colocalizes with the nucleus (Hoechst staining shown as green); the projection even exaggerates the true amount of nuclear LSm1, as it includes a thin layer of cytoplasm underneath and above the nucleus (not depicted). ActD treatment, instead, significantly increases the amount of LSm1 in the nucleus (Fig. 7 A, bottom). Because of the variability between cells (see beginning of paragraph), we wanted to confirm the data by performing a statistical analysis. LSm1 signal that colocalized with the nucleus was quantified and normalized first to the area of the nuclear projection and then to the mean LSm1 nuclear staining in the control samples. As shown in Fig. 7 B, ActD induces a twofold increase in the mean nuclear LSm1 signal ($n = 6$; $P < 0.05$ in Student's t test). We conclude that LSm1 clearly has a nuclear phase. Although we cannot exclude collateral effects of the ActD treatment, the significant increase in nuclear LSm1 is in agreement with the hypothesis that LSm1 exits the nucleus together with newly formed mRNPs.

Translation of some dendritic mRNAs is activated upon synaptic stimulation, and a hallmark of this activation is the concomitant migration of mRNP components into the stimulated spines (see Introduction). We therefore tested whether synaptic stimulation leads to a redistribution of LSm1. Indeed, a 5-min treatment with (S)-3,5-dihydroxyphenylglycine (DHPG) causes a significant increase of both the LSm1 and CBP80 signal in the dendrites of primary hippocampal neurons. To verify that the dendrites carry functional synapses, we performed a triple staining with an α-synaptophysin antibody that marks presynaptic sites (Fig. 8, A and B, top rows), phalloidin that highlights points of F-actin enrichment and hence dendrites (second rows), and α-LSm1 or α-CBP80 antibodies (third rows). A mask was created using a dedicated algorithm (see Materials and methods), which marks all the points in the image that are within a 0.4-µm

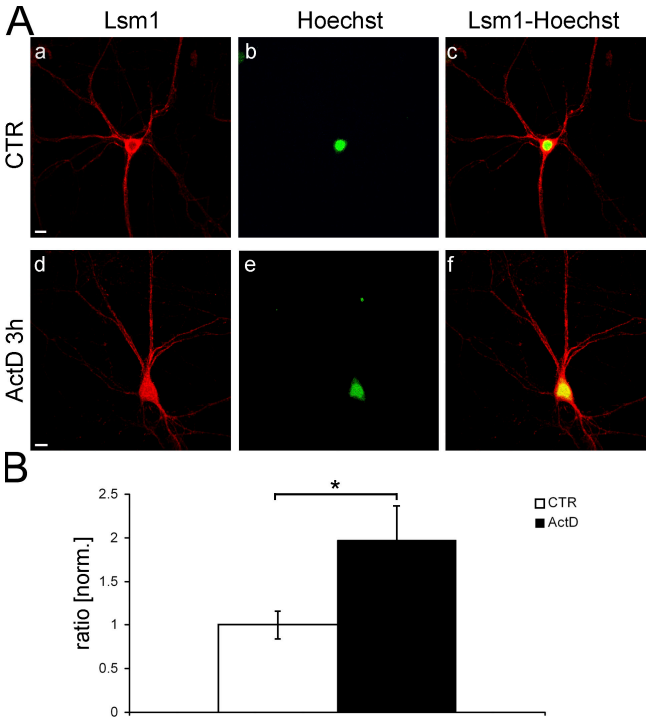

Figure 7. **ActD treatment enhances LSm1 staining in the nucleus.** (A) Control hippocampal neurons (18 DIV; a–c) or hippocampal neurons treated for 3 h with ActD (18 DIV; d–f) were stained with α-LSm1 antibodies (a and d) and Hoechst (b and e). A stack of 8–12 optical slices was recorded at the confocal microscope. Shown is the projection of all slices using the Z project algorithm. Panels c and f show the overlay of the LSm1 and the Hoechst staining. Bars, 10 µm. (B) LSm1 colocalization with the nucleus of six neurons was quantified and normalized for the area of the nucleus. Shown is the mean intensity in the control nuclei (arbitrarily set to 1) and in the ActD-treated nuclei. Error bars indicate the standard error. *, $P < 0.05$ in Student's t test.

distance from both synaptophysin-positive foci and sites of F-actin enrichment, i.e., that are in close vicinity to a functional synapse. The mask is shown in green in the fourth row (Fig. 8, A and B). As is evident from the picture, some LSm1 signal (Fig. 8, A and B, fourth row, red) is found in the vicinity of untreated synapses (left) and therefore appears yellow in the merged picture (arrows). After DHPG treatment, the signal within the mask increased (Fig. 8, A and B, right). Statistical evaluation of at least 30 neurons for each condition confirmed the data: the LSm1 signal in vicinity of the synapses increased by 44% ($P < 0.001$; Fig. 8 C) and CBP80 by 30% ($P < 0.01$). We therefore conclude that both LSm1 and CBP80 move into the spines upon stimulation, which is highly indicative that translation of LSM1/CBP80 mRNPs is activated.

Discussion

In this paper, we describe the composition of an mRNP that is localized in the dendrites of various types of neurons in vitro and in vivo. Three characteristics of this mRNP are remarkable. First, it contains the LSm proteins LSm1 and LSm4, and presumably five other LSm proteins as well, to complete the heptamer (see Introduction). LSm proteins are auxiliary factors of mRNA decapping in yeast and components of the P bodies in

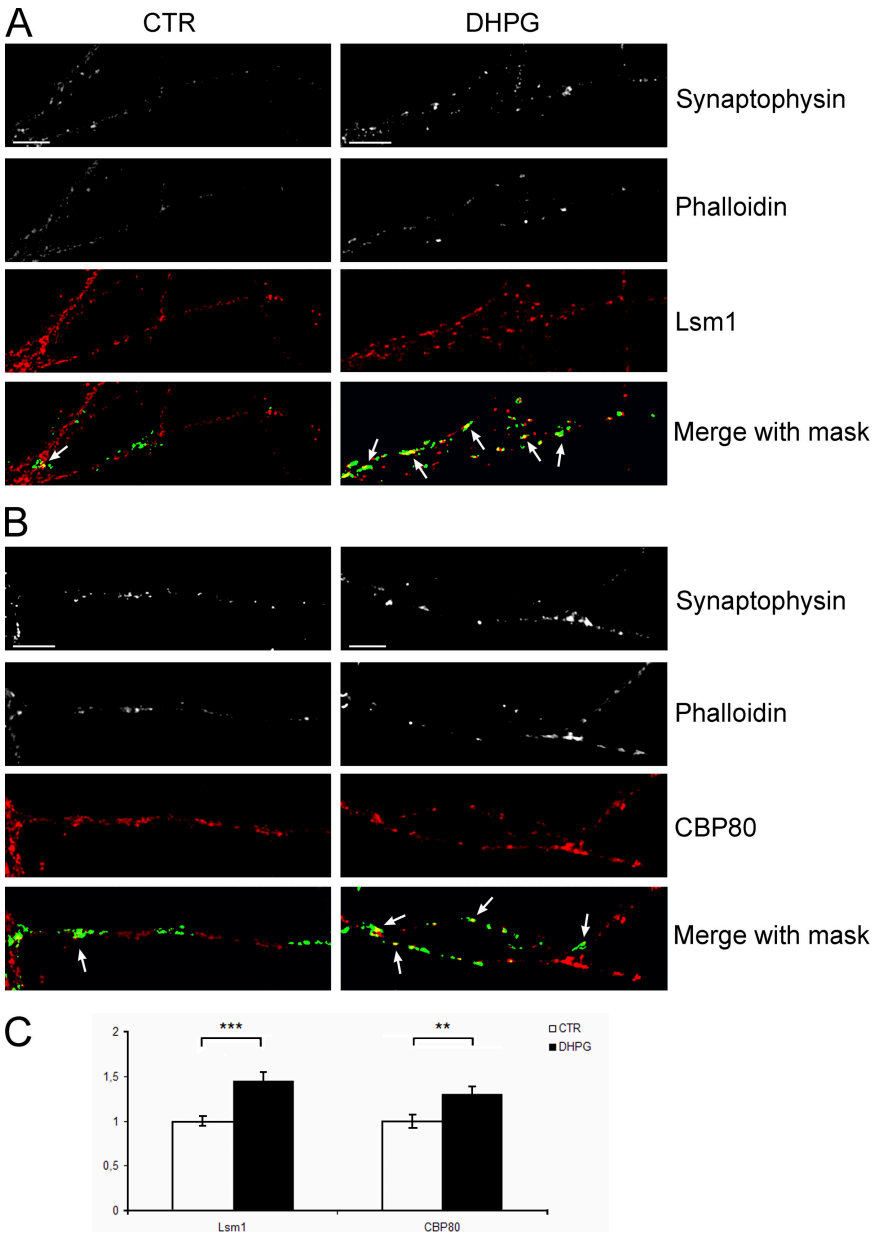

Figure 8. **DHPG stimulation causes a relocalization of LSm1 toward the synapses.** (A) Hippocampal cells were fixed directly (left) or after a 5-min stimulation with DHPG in the medium (right). Cells were stained with α-synaptophysin (top), with phalloidin (second row), as well as with polyclonal α-LSm1 (third row). Shown are single optical slices taken on the confocal microscope: the top three rows show the single channels and the bottom row shows a picture that merges the red channel of LSm1 with a mask that highlights the synapses and the surrounding area to a distance of ~0.4 μm (green). Synapses appear mostly green in the control, but much more yellow after stimulation (arrows). (B) As in A, but stained with α-CBP80 antibodies instead of α-LSm1. Bars, 10 μm. (C) LSm1 and CBP80 immunofluorescence intensity, respectively, that fell inside the synapses mask was integrated for at least 30 neurons of 16–18 DIV and was normalized first for the area and then for the average control without DHPG stimulation. The resulting values and the significance according to Student's *t* test are shown (**, $P < 0.01$; ***, $P < 0.001$).

all eukaryotes (see Introduction). In neuronal dendrites, instead, LSm1 associates with stable mRNPs that can be isolated and characterized. The presence of an intact poly(A) tail (Fig. 5) and a m^7G cap (as indicated by the presence of a cap-binding factor; Fig. 5) further support the notion that the respective mRNAs are not undergoing degradation. The presence of LSm1 in these neuronal mRNPs further underlines the overlap between the various types of RNA granules, P bodies and stress granules in cell lines, maternally stored mRNPs in *Drosophila melanogaster* oocytes, and neuronal transport mRNPs (Anderson and Kedersha, 2006). The oskar mRNP in *Drosophila* oocytes (Lin et al., 2006) and neuronal Staufen-containing transport mRNPs (Barbee et al., 2006) contain the decapping enzyme Dcp1/Dcp1a even when their function does not involve mRNA degradation, indicating that the different functions of the P body–type granules are not physically separated. The mammalian neuronal LSm1 protein, instead, coincides with the Dcp1a-decapping enzyme only in the cell body. In the dendrites, the two proteins segregate (Fig. 6), indicating that mRNA degradation and LSm1-associated mRNP localization are separated in space. This notion is further supported by the absence of Dcp1a in purified LSm1 particles (Fig. 5). Therefore the neuronal mRNP granules are heterogeneous, at least in mammalian neurons, in that dendritic LSm1-mRNPs and P bodies are distinct.

In the central nervous system, we observed LSm1 in neuronal dendrites (Figs. 1 and 2), but expression levels vary widely, with dendrites of pyramidal neurons and especially of Purkinje cells labeled most. The selectivity is even more pronounced when looking at axonal processes: in the brain, we could not detect LSm1 in axonal fibers or presynaptic structures. In the spinal cord, instead, fibers that can be anatomically defined as axonal projections, most likely of the α-motor neurons, are clearly LSm1 positive (Fig. 2). LSm1 thus appears to have a function that is either specific for certain neuron subtypes or

that requires more LSm1 in certain neurons than in others. This is remarkable with respect to the interaction of the LSm proteins with the SMN protein in vitro (Brahms et al., 2001; Friesen et al., 2001) and in brain extracts (Fig. 5): because of the selective effect of SMN depletion on α-motor neurons, it has been hypothesized that the protein may have a neuron-specific role in addition to its housekeeping function (Sendtner, 2001). Further, the primary defect in the motor neurons is a failure to mature and/or maintain the axonal projection. The LSm complex might therefore be the missing link between SMN insufficiency and motor neuron degeneration.

LSm1 has been primarily described as an auxiliary mRNA degradation factor. Detailed analysis in yeast shows that Lsm1p regulates translation (Holmes et al., 2004) and the LSm1-associated factor Pat1p inhibits translation initiation (Coller and Parker, 2005). Similarly, mammalian LSm acts upstream of the degrading enzymes hDcp1a and hXrn1 (Cougot et al., 2004; Andrei et al., 2005). We therefore believe that the neuronal LSm1 mRNPs will also be translationally silent. An indication of this is the size distribution of LSm1 on sucrose gradients does not follow a typical "polysome" profile, with a second peak of more than 80S. More importantly, the mRNP contains the nuclear cap-binding protein, strongly indicating that the mRNA has not yet undergone its pioneer round of translation (see next paragraph). LSm1 mRNPs associate with the small ribosomal subunit, whereas no significant amounts of the large subunit were observed (Fig. 5), which might hint at the possibility that the LSm1 mRNPs represent stalled 48S preinitiation complexes. They may in this respect resemble transport mRNPs that form around the zip-code binding protein ZBP1, in which parts of the small, but not of the large ribosomal subunit have been detected (Jønson et al., 2007). Consistently, ZBP1 inhibits translation at the 48S stage (Hüttelmaier et al., 2005).

Remarkably, the LSm1 mRNPs contain the "nuclear" cap-binding protein CBP80 instead of the translation initiation factor eIF4E. This protein binds to mRNA precursors in the nucleus (Izaurralde et al., 1994) and remains bound to the mRNA throughout its maturation and export from the nucleus (Visa et al., 1996). In the cytoplasm, CBP80 is removed in a pioneer round of translation and eIF4E takes its place (Ishigaki et al., 2001; Lejeune et al., 2002). CBP80 so far has not been implicated in neuronal mRNA transport. Here we show that CBP80 is present along the dendrites (Figs. 6). mGluR-mediated translational stimulation causes a significant shift of CBP80 toward the synapses, which is a hallmark of the activation of local protein synthesis (Fig. 8). These findings together strongly suggest that CBP80 has a role during dendritic mRNP transport.

First of all, this implies that the respective mRNAs have not yet undergone the pioneer round of translation when they are transported into the dendrites. Quite possibly, they were committed for dendritic transport already in the nucleus (see also below). While this study was under way, it was reported that components of the exon junction complex are also found in the dendrites (Giorgi et al., 2007). The exon junction complex is deposited onto the mRNA in the nucleus and is likewise stripped off the mRNA by the pioneer round of translation, and this observation is therefore compatible with the idea of an early commitment to transport. A nuclear commitment to cytoplasmic transport has been shown before for the *oskar* mRNAs in *Drosophila* oocytes (Hachet and Ephrussi, 2004) and may also play a role in *Xenopus laevis* oocytes (Kress et al., 2004). The ZBP1 transport mRNP in HEK cells also contains CBP80 (Jønson et al., 2007), suggesting that the nuclear history of mRNA transport is a wide-spread phenomenon. LSm1 is regarded as a cytoplasmic protein. Contrary to this belief, primary neurons have a variable fraction of the protein in the nucleus, and inhibition of ex novo formation of mRNPs by transcription repression significantly increases the nuclear LSm1 fraction (Fig. 7). This gives a first indication that LSm1 can shuttle between the nucleus and the cytoplasm, with the nuclear export depending on mRNP export, and the LSm1/CBP80 mRNP could well assemble in the nucleus.

Finally, the LSm1 mRNPs associate with CPEB (Fig. 5). CPEB binds to the cytoplasmic polyadenylation element that is present on some mRNAs and can trigger, upon glutamergic stimulation, elongation of the poly(A) tails and hence translation activation of the respective mRNPs (Wu et al., 1998; Wells et al., 2001). CPEB is present at the dendrites and enters into the spines upon synaptic stimulation (Huang et al., 2003), similar to what we observe for LSm1 and CBP80. Our poly(A) tail length measurement shows that LSm1-associated mRNAs are not deadenylated; only a subpopulation of the β-actin mRNA might be. There are two possible interpretations: CPEB might have a role in dendritic mRNA transport beyond poly(A) length control (e.g., CPEB is present on mRNPs during transport [Huang et al., 2003]) and/or only a subset of the LSm1-associated mRNAs, whose identity we do not currently know, contain critically short poly(A) tails so that their translational activation requires cytoplasmic polyadenylation.

The model that emerges from our data is depicted in Fig. 9. LSm1 and CBP80 assemble in the nucleus onto mRNPs that are destined to be transported into the dendrites. Likely, the pioneer round of translation is initiated, but then blocked at the 48S pre-translation complex. It remains to be seen at what stage CPEB joins the complex; the fact that it is present during transport along the dendrites (Huang et al., 2003) implies that it also enters at an early time point. All the key players in this mRNP have been shown previously or in this manuscript to be present at the dendrites, and it is therefore straightforward to assume that they are part of the migrating mRNP. Finally, at least LSm1 and CBP80 shift into the dendritic spines when the synapses are stimulated, which is causing translational activation. We cannot exclude the possibility that translation then takes place in the presence of both factors, e.g., by internal ribosomal entry site–mediated translation initiation (Pinkstaff et al., 2001), but we think it is more likely they are replaced in loco to give way for normal, eIF4E-dependent translation (Smart et al., 2003). This model sheds new light on the dendritic targeting and transport of mRNPs and will thus be an important stimulus for future studies.

Materials and methods

All animal experiments in this study were performed using Wistar rats and C56/BL6 mice (Harlan or Charles River Laboratories) that were

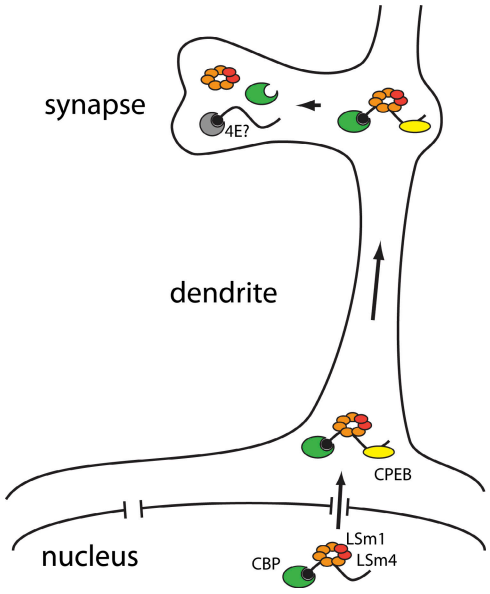

Figure 9. **Model.** mRNPs bound for dendritic transport associate with the LSm complex already in the nucleus, with the nuclear cap-binding protein still attached. Whether CPEB joins the complex also in the nucleus, or only after export, remains to be elucidated. The mRNP carrying these markers is then found in the dendrite and is shifted as such into stimulated dendritic spines. There, the mRNA is presumably liberated to allow eIF4E-dependent translation.

group-housed in standard cages and kept under a 12-h light/dark cycle with food and water ad libitum. All animal experiments were performed in accordance to the Italian law on the use and care of laboratory animals (DL 116\92).

The antibodies used in this study were as follows: affinity-purified rabbit α-LSm1 and α-LSm4 (Ingelfinger et al., 2002); mouse SMI31 and SMI32 (Sternberger); mouse α-Calbindin (Swant); mouse α-glial fibrillary acidic protein (Sigma-Aldrich); mouse α-synaptophysin (Millipore); rabbit α-CPEB1 (gift from D. Wells, Yale University, New Haven, CT); mouse α-MAP2 (Sigma-Aldrich); α-SMN (Signal Transduction); mouse α-eIF4E (Santa Cruz Biotechnology, Inc.); goat α-orexin (Santa Cruz Biotechnology, Inc.); rabbit α-Dcp1a (gift from J. Lykke-Andersen, University of Colorado, Boulder, CO); rabbit α-rS6 and α-L11 (gift from F. Lorreni, University of Rome, Rome, Italy); and rabbit α-CBP80 (gift from I. Mattaj, European Molecular Biology Laboratory, Heidelberg, Germany).

For neuronal transfections, the CMV promoter of pcDNA3 was replaced with a cassette of the rat tubulin α1 promoter (position −989 to +93; Gloster et al., 1994) and the yellow fluorescent YPet protein (Nguyen and Daugherty, 2005). Downstream of YPet, the ORFs encoding LSm1, LSm4 (Ingelfinger et al., 2002), and Dcp1a (amplified from cDNA using primers based on Lykke-Andersen, 2002) were inserted; the integrity of the ORFs was verified by sequencing.

Primary neuron culture and immunofluorescence analysis

Spinal cords were obtained from embryonic day 12–14 fetal rats. After removal of the dorsal root ganglia, 10–14 spinal cords were dissected, washed with 5 ml of Earl's Balanced Salt Solution, and centrifuged for 2 min at 150 *g*. The tissue was resuspended and incubated for 15 min at 37°C with 0.02% trypsin followed by addition of DNase I (80 µg/ml final) and trypsin inhibitor (0.52 mg/ml). Digested tissues were mechanically dissociated and centrifuged at 150 *g* for 10 min. The dissociated cells were plated at a density of 12 × 10^4 cells/cm^2 in MEM (Invitrogen) supplemented with 10% heat-inactivated FBS or in Neurobasal media (Invitrogen) supplemented with B27. Rat Purkinje cells were obtained from postnatal day 7 rat cerebellum as described previously (Gallo et al., 1982).

Hippocampal neuron cultures were prepared from an embryonic day 19 mouse. The brains were removed and hippocampi were freed of meninges, treated with 0.025% trypsin, minced, and plated on poly-L-lysine (Sigma-Aldrich) wells in Neurobasal supplemented with 2% B27. Neurons were maintained at 37°C and 5% CO_2. For drug treatment, cells were treated at 16–18 d in vitro (DIV) before fixation with 10 µg/ml actinomycin D for 3 h (ActD; Sigma-Aldrich) or with 100 µM DHPG for 5 min (Sigma-Aldrich). Cells were transfected with calcium phosphate precipitations at 10 DIV. In brief, 4 µg DNA were mixed with calcium chloride and precipitated with HBSS phosphate buffer (PB). The microprecipitates were applied to the cells for 45 min, and then washed off. Cells were fixed and stained after 20 h of expression.

For immunofluorescence analysis, cells were fixed with 2% PFA, permeabilized with 0.2% Triton X-100, and blocked with 10% FBS in PBS. Fixed cells were incubated for 1 h at room temperature with the primary antibodies diluted in 10% FBS in PBS. The cells were washed three times with PBS and incubated for 1 h at room temperature with Cy2-conjugated α-mouse IgG and Cy3-conjugated α-rabbit IgG secondary antibodies (GE Healthcare) and washed again three times with PBS. Where applicable, cells were stained with 50 µg/ml phalloidin-FITC conjugate (Sigma-Aldrich) in PBS for 25 min at RT and washed three times. Transfections were counterstained using Pacific blue–conjugated secondary antibodies. Coverslips were embedded in Mowiol (EMD) or Gelmount (Biomeda). Images were recorded using the confocal scanning microscope (LSM 510 [Carl Zeiss, Inc.], 63/1.4 objective, or Radiance 2100 [Bio-Rad Laboratories], 60/1.4 objective) and analyzed using the Carl Zeiss, Inc. software as well as the ImageJ program (version 1.40). The mask to identify active synapses and surrounding areas was generated on the basis of spatial correlation of the synaptophysin and the phalloidin staining, large accumulations were discarded from analysis to prevent misinterpretations. In brief, an algorithm was realized with the ImageJ package and the JACoP plug-in (Bolte and Cordelières, 2006; http://rsb.info.nih.gov/ij/) that takes the overlap of presynaptic and postsynaptic signal and enlarges it three times by one pixel. In this way, areas within ∼400 nm or less were identified as synapses.

Tissue preparation and immunofluorescence staining

Three adult male rats weighing 200–250 g were transcardially perfused under deep anesthesia (60 mg/kg Nembutal i.p.) with 150 ml of 0.9% saline at room temperature followed by 200 ml of cold 4% PFA in 0.1 M PB, pH 7.4. Brains were dissected, postfixed for 2 h at room temperature, and cryoprotected in 30% sucrose/PB at 4°C. They were then frozen with dry ice and cut into 40-µm transverse sections with a freezing microtome. All antibody solutions were prepared in PB and 0.3% Triton X-100 and incubated overnight at room temperature. After incubation with the cocktail of primary antibodies, the sections were washed three times in PB and subsequently incubated for 2 h at room temperature in a cocktail of Cy2-conjugated donkey α-mouse IgG and Cy3-conjugated donkey α-rabbit IgG secondary antibodies (1:100 each; Jackson ImmunoResearch Laboratories). Sections were washed three times in PB, mounted on gelatin-coated slides, and coverslipped in Gelmount (Biomeda). Anatomical boundaries and nomenclature were named according to Paxinos and Watson (1994). Images were acquired on a confocal microscope (10/0.3, 20/0.5, and 63/1.4 objectives) and exported in JPEG format; the contrast and brightness were adjusted and final plates were composed with Adobe Illustrator 9 or Corel Draw 9.

Rat brain extracts and immunoprecipitation

Whole brain (postnatal day 1 or 2 rats) was homogenized by dounce homogenization in 3 ml/brain of ice-cold IMAC buffer (Kanai et al., 2004) in the presence of 0.1 mM PMSF. The lysate was centrifuged at 15,000 *g* for 5 min at 4°C. Supernatants were pooled and total protein concentration was estimated by the Bradford assay (Bio-Rad Laboratories). For immunoprecipitations, brain lysate (750 µg of total protein) in 300 µl IP buffer (150 mM NaCl, 20 mM Tris-Cl, pH 7.5, and 0.1% Triton X-100) were precipitated with 20 µl of affinity-purified α-LSm1 antibodies immobilized on protein A–Sepharose (GE Healthcare). After washing with IP buffer, bound proteins were eluted with SDS loading buffer, resolved by SDS-PAGE, and analyzed by Western blotting, using the enhanced chemiluminescence detection system (GE Healthcare).

For cross-linking experiments, a postnatal day 2 rat brain was minced, divided into equal parts, and irradiated with a germicidal lamp for 0, 45, and 90 s. After irradiation, the tissue was homogenized in 1 ml RIPA buffer (150 mM NaCl, 50 mM Tris-Cl, pH 7.5, 1% NP-40, and 1% DOC), and the extract was cleared by centrifugation. Immunoprecipitation was performed as described above using RIPA buffer for the washes.

To reduce the RNA background in immunoprecipitation/RT-PCR experiments, the brain lysate was precleared in such experiments for 1 h with 20 µl protein A–Sepharose (preblocked with 0.3% BSA in PBS and 100 µg/ml of *Escherichia coli* tRNA); otherwise, the immunoprecipitation was performed as above using IP buffer in the wash steps. Bound RNAs

were eluted in elution buffer (0.2 M NaOAc, pH 5.2, 0.2% SDS, and 1 mM EDTA), purified by phenol-chloroform extraction, and concentrated by ethanol precipitation. cDNAs were synthesized using p(dN_6) and M-MuLV reverse transcription (New England BioLabs, Inc.) in 20 µl of reaction volume as described by the manufacturer. 2 µl of the reaction mixture was used in standard PCR reactions using Taq polymerase (New England Biolabs, Inc.). Primers are listed in Table S1 (available at http://www.jcb.org/cgi/content/full/jcb.200807033/DC1).

In the coupled sucrose gradient/immunoprecipitation experiments, brain lysate equivalent to 2.5 mg of total protein was loaded onto each SW41 tube with a 10–45% sucrose gradient, prepared in 10 mM Hepes-KOH, pH 7.5, and 150 mM KOAc, and centrifuged at 40,000 rpm for 2 h and 10 min. After harvesting the gradient, the respective fractions of four to six gradient tubes were pooled and Triton X-100 was added to 0.1%. It was then incubated for 1 h at 4°C with the respective antibodies immobilized to 150 µl of protein A–Sepharose. The beads were washed three times with 10 mM Hepes-KOH, pH 7.5, 150 mM KOAc, and 0.1% Triton X-100, and bound complexes were eluted with elution buffer. RNAs and proteins were recovered by EtOH and acetone precipitation, respectively, and analyzed as before. The tag-addition poly(A) test method is described in detail in Fig. S2.

Online supplemental material

Fig. S1 shows the specificity of the anti-LSm1 antibodies. Fig. S2 shows further regions of the central nervous system stained for LSm1. Fig. S3 explains and shows the validation of the poly(A) test method. Table S1 lists all the primers used in the study and the exon they anneal to. Online supplemental material is available at http://www.jcb.org/cgi/content/full/jcb.200807033/DC1.

We thank David Wells, Iain Mattaj, Jens Lykke-Andersen, and Fabrizio Loreni for the gift of antibodies and the laboratory of Carlos Dotti at the Flanders Institute for Biotechnology for one set of mouse hippocampal neurons. We further thank Fabrizio Renzi for help with the construction of the transfection plasmids.

This study was supported by the Italian Ministry of Health (Progetto Finalizzato), by the Italian Ministry of Universities (Fondo per gli Investimenti della Ricerca di Base), by the Flanders Institute for Biotechnology (VIB), and by a Methusalem grant to Bart De Strooper (Katholieke Universiteit, Leuven).

Submitted: 7 July 2008
Accepted: 7 January 2009

References

Achsel, T., H. Brahms, B. Kastner, A. Bachi, M. Wilm, and R. Lührmann. 1999. A doughnut-shaped heteromer of human Sm-like proteins binds to the 3′-end of U6 snRNA, thereby facilitating U4/U6 duplex formation in vitro. *EMBO J.* 18:5789–5802.

Anderson, P., and N. Kedersha. 2002. Stressful initiations. *J. Cell Sci.* 115:3227–3234.

Anderson, P., and N. Kedersha. 2006. RNA granules. *J. Cell Biol.* 172:803–808.

Andrei, M.A., D. Ingelfinger, R. Heintzmann, T. Achsel, R. Rivera-Pomar, and R. Lührmann. 2005. A role for eIF4E and eIF4E-transporter in targeting mRNPs to mammalian processing bodies. *RNA.* 11:717–727.

Bagni, C., and W.T. Greenough. 2005. From mRNP trafficking to spine dysmorphogenesis: the roots of fragile X syndrome. *Nat. Rev. Neurosci.* 6:376–387.

Barbee, S.A., P.S. Estes, A.M. Cziko, J. Hillebrand, R.A. Luedeman, J.M. Coller, N. Johnson, I.C. Howlett, C. Geng, R. Ueda, et al. 2006. Staufen- and FMRP-containing neuronal RNPs are structurally and functionally related to somatic P bodies. *Neuron.* 52:997–1009.

Bolte, S., and F.P. Cordelières. 2006. A guided tour into subcellular colocalization analysis in light microscopy. *J. Microsc.* 224:213–232.

Brahms, H., L. Meheus, V. de Brabandere, U. Fischer, and R. Lührmann. 2001. Symmetrical dimethylation of arginine residues in spliceosomal Sm protein B/B' and the Sm-like protein LSm4, and their interaction with the SMN protein. *RNA.* 7:1531–1542.

Brengues, M., D. Teixeira, and R. Parker. 2005. Movement of eukaryotic mRNAs between polysomes and cytoplasmic processing bodies. *Science.* 310:486–489.

Coller, J., and R. Parker. 2005. General translational repression by activators of mRNA decapping. *Cell.* 122:875–886.

Cougot, N., S. Babajko, and B. Seraphin. 2004. Cytoplasmic foci are sites of mRNA decay in human cells. *J. Cell Biol.* 165:31–40.

Ferrari, F., V. Mercaldo, G. Piccoli, C. Sala, S. Cannata, T. Achsel, and C. Bagni. 2007. The fragile X mental retardation protein-RNP granules show an mGluR-dependent localization in the post-synaptic spines. *Mol. Cell. Neurosci.* 34:343–354.

Filipowicz, W., S.N. Bhattacharyya, and N. Sonenberg. 2008. Mechanisms of post-transcriptional regulation by microRNAs: are the answers in sight? *Nat. Rev. Genet.* 9:102–114.

Friesen, W.J., and G. Dreyfuss. 2000. Specific sequences of the Sm and Sm-like (Lsm) proteins mediate their interaction with the spinal muscular atrophy disease gene product (SMN). *J. Biol. Chem.* 275:26370–26375.

Friesen, W.J., S. Massenet, S. Paushkin, A. Wyce, and G. Dreyfuss. 2001. SMN, the product of the spinal muscular atrophy gene, binds preferentially to dimethylarginine-containing protein targets. *Mol. Cell.* 7:1111–1117.

Gallo, V., M.T. Ciotti, A. Coletti, F. Aloisi, and G. Levi. 1982. Selective release of glutamate from cerebellar granule cells differentiating in culture. *Proc. Natl. Acad. Sci. USA.* 79:7919–7923.

Giorgi, C., G.W. Yeo, M.E. Stone, D.B. Katz, C. Burge, G. Turrigiano, and M.J. Moore. 2007. The EJC factor eIF4AIII modulates synaptic strength and neuronal protein expression. *Cell.* 130:179–191.

Gloster, A., W. Wu, A. Speelman, S. Weiss, C. Causing, C. Pozniak, B. Reynolds, E. Chang, J.G. Toma, and F.D. Miller. 1994. The T alpha 1 alpha-tubulin promoter specifies gene expression as a function of neuronal growth and regeneration in transgenic mice. *J. Neurosci.* 14:7319–7330.

Hachet, O., and A. Ephrussi. 2004. Splicing of oskar RNA in the nucleus is coupled to its cytoplasmic localization. *Nature.* 428:959–963.

Holmes, L.E., S.G. Campbell, S.K. De Long, A.B. Sachs, and M.P. Ashe. 2004. Loss of translational control in yeast compromised for the major mRNA decay pathway. *Mol. Cell. Biol.* 24:2998–3010.

Huang, Y.S., J.H. Carson, E. Barbarese, and J.D. Richter. 2003. Facilitation of dendritic mRNA transport by CPEB. *Genes Dev.* 17:638–653.

Hüttelmaier, S., D. Zenklusen, M. Lederer, J. Dictenberg, M. Lorenz, X. Meng, G.J. Bassell, J. Condeelis, and R.H. Singer. 2005. Spatial regulation of beta-actin translation by Src-dependent phosphorylation of ZBP1. *Nature.* 438:512–515.

Iijima, T., T. Imai, Y. Kimura, A. Bernstein, H.J. Okano, M. Yuzaki, and H. Okano. 2005. Hzf protein regulates dendritic localization and BDNF-induced translation of type 1 inositol 1,4,5-trisphosphate receptor mRNA. *Proc. Natl. Acad. Sci. USA.* 102:17190–17195.

Ingelfinger, D., D.J. Arndt-Jovin, R. Lührmann, and T. Achsel. 2002. The human LSm1-7 proteins colocalize with the mRNA-degrading enzymes Dcp1/2 and Xrnl in distinct cytoplasmic foci. *RNA.* 8:1489–1501.

Ishigaki, Y., X. Li, G. Serin, and L.E. Maquat. 2001. Evidence for a pioneer round of mRNA translation: mRNAs subject to nonsense-mediated decay in mammalian cells are bound by CBP80 and CBP20. *Cell.* 106:607–617.

Izaurralde, E., J. Lewis, C. McGuigan, M. Jankowska, E. Darzynkiewicz, and I.W. Mattaj. 1994. A nuclear cap binding protein complex involved in pre-mRNA splicing. *Cell.* 78:657–668.

Jønson, L., J. Vikesaa, A. Krogh, L.K. Nielsen, T.V. Hansen, R. Borup, A.H. Johnsen, J. Christiansen, and F.C. Nielsen. 2007. Molecular composition of IMP1 RNP granules. *Mol. Cell. Proteomics.* 6:798–811.

Kanai, Y., N. Dohmae, and N. Hirokawa. 2004. Kinesin transports RNA: isolation and characterization of an RNA-transporting granule. *Neuron.* 43:513–525.

Köhrmann, M., M. Luo, C. Kaether, L. DesGroseillers, C.G. Dotti, and M.A. Kiebler. 1999. Microtubule-dependent recruitment of Staufen-green fluorescent protein into large RNA-containing granules and subsequent dendritic transport in living hippocampal neurons. *Mol. Biol. Cell.* 10:2945–2953.

Kress, T.L., Y.J. Yoon, and K.L. Mowry. 2004. Nuclear RNP complex assembly initiates cytoplasmic RNA localization. *J. Cell Biol.* 165:203–211.

Lejeune, F., Y. Ishigaki, X. Li, and L.E. Maquat. 2002. The exon junction complex is detected on CBP80-bound but not eIF4E-bound mRNA in mammalian cells: dynamics of mRNP remodeling. *EMBO J.* 21:3536–3545.

Lin, M.D., S.J. Fan, W.S. Hsu, and T.B. Chou. 2006. *Drosophila* decapping protein 1, dDcp1, is a component of the oskar mRNP complex and directs its posterior localization in the oocyte. *Dev. Cell.* 10:601–613.

Lykke-Andersen, J. 2002. Identification of a human decapping complex associated with hUpf proteins in nonsense-mediated decay. *Mol. Cell. Biol.* 22:8114–8121.

Martin, K.C., and R.S. Zukin. 2006. RNA trafficking and local protein synthesis in dendrites: an overview. *J. Neurosci.* 26:7131–7134.

Meister, G., C. Eggert, and U. Fischer. 2002. SMN-mediated assembly of RNPs: a complex story. *Trends Cell Biol.* 12:472–478.

Mendez, R., and J.D. Richter. 2001. Translational control by CPEB: a means to the end. *Nat. Rev. Mol. Cell Biol.* 2:521–529.

Meyer, S., C. Temme, and E. Wahle. 2004. Messenger RNA turnover in eukaryotes: pathways and enzymes. *Crit. Rev. Biochem. Mol. Biol.* 39:197–216.

Napoli, I., V. Mercaldo, P. Pilo Boyl, B. Eleuteri, F. Zalfa, S. De Rubeis, D. Di Marino, E. Mohr, M. Massimi, M. Falconi, et al. 2008. The fragile X syndrome protein represses activity-dependent translation through CYFIP1, a new 4E-BP. *Cell.* 134:1042–1054.

Nguyen, A.W., and P.S. Daugherty. 2005. Evolutionary optimization of fluorescent proteins for intracellular FRET. *Nat. Biotechnol.* 23:355–360.

Ostroff, L.E., J.C. Fiala, B. Allwardt, and K.M. Harris. 2002. Polyribosomes redistribute from dendritic shafts into spines with enlarged synapses during LTP in developing rat hippocampal slices. *Neuron.* 35:535–545.

Paxinos, G., and C. Watson. 1994. The Rat Brain in Stereotaxis Coordinates. Academic Press, Sydney. 438 pp.

Pinkstaff, J.K., S.A. Chappell, V.P. Mauro, G.M. Edelman, and L.A. Krushel. 2001. Internal initiation of translation of five dendritically localized neuronal mRNAs. *Proc. Natl. Acad. Sci. USA*. 98:2770–2775.

Piper, M., and C. Holt. 2004. RNA translation in axons. *Annu. Rev. Cell Dev. Biol.* 20:505–523.

Sendtner, M. 2001. Molecular mechanisms in spinal muscular atrophy: models and perspectives. *Curr. Opin. Neurol.* 14:629–634.

Seydoux, G. 1996. Mechanisms of translational control in early development. *Curr. Opin. Genet. Dev.* 6:555–561.

Smart, F.M., G.M. Edelman, and P.W. Vanderklish. 2003. BDNF induces translocation of initiation factor 4E to mRNA granules: evidence for a role of synaptic microfilaments and integrins. *Proc. Natl. Acad. Sci. USA.* 100:14403–14408.

Steward, O., and E.M. Schuman. 2003. Compartmentalized synthesis and degradation of proteins in neurons. *Neuron.* 40:347–359.

Tharun, S., and R. Parker. 2001. Targeting an mRNA for decapping: displacement of translation factors and association of the Lsm1p-7p complex on deadenylated yeast mRNAs. *Mol. Cell.* 8:1075–1083.

Tharun, S., W. He, A.E. Mayes, P. Lennertz, J.D. Beggs, and R. Parker. 2000. Yeast Sm-like proteins function in mRNA decapping and decay. *Nature.* 404:515–518.

Tsokas, P., E.A. Grace, P. Chan, T. Ma, S.C. Sealfon, R. Iyengar, E.M. Landau, and R.D. Blitzer. 2005. Local protein synthesis mediates a rapid increase in dendritic elongation factor 1A after induction of late long-term potentiation. *J. Neurosci.* 25:5833–5843.

Ule, J., K.B. Jensen, M. Ruggiu, A. Mele, A. Ule, and R.B. Darnell. 2003. CLIP identifies Nova-regulated RNA networks in the brain. *Science.* 302:1212–1215.

Vessey, J.P., A. Vaccani, Y. Xie, R. Dahm, D. Karra, M.A. Kiebler, and P. Macchi. 2006. Dendritic localization of the translational repressor Pumilio 2 and its contribution to dendritic stress granules. *J. Neurosci.* 26:6496–6508.

Villacé, P., R.M. Marión, and J. Ortín. 2004. The composition of Staufen-containing RNA granules from human cells indicates their role in the regulated transport and translation of messenger RNAs. *Nucleic Acids Res.* 32:2411–2420.

Visa, N., E. Izaurralde, J. Ferreira, B. Daneholt, and I.W. Mattaj. 1996. A nuclear cap-binding complex binds Balbiani ring pre-mRNA cotranscriptionally and accompanies the ribonucleoprotein particle during nuclear export. *J. Cell Biol.* 133:5–14.

Wells, D.G., X. Dong, E.M. Quinlan, Y.S. Huang, M.F. Bear, J.D. Richter, and J.R. Fallon. 2001. A role for the cytoplasmic polyadenylation element in NMDA receptor-regulated mRNA translation in neurons. *J. Neurosci.* 21:9541–9548.

Wu, L., D. Wells, J. Tay, D. Mendis, M.A. Abbott, A. Barnitt, E. Quinlan, A. Heynen, J.R. Fallon, and J.D. Richter. 1998. CPEB-mediated cytoplasmic polyadenylation and the regulation of experience-dependent translation of alpha-CaMKII mRNA at synapses. *Neuron.* 21:1129–1139.

Zhang, H.L., T. Eom, Y. Oleynikov, S.M. Shenoy, D.A. Liebelt, J.B. Dictenberg, R.H. Singer, and G.J. Bassell. 2001. Neurotrophin-induced transport of a beta-actin mRNP complex increases beta-actin levels and stimulates growth cone motility. *Neuron.* 31:261–275.